

Chamotte Clay: A Natural Adsorbent for Separation and Preconcentration of Aluminium

Raif İLKTAÇ 

Application and Research Center for Testing and Analysis, University of Ege, 35100 Bornova, İzmir, Türkiye

Received: 25/08/2022, **Revised:** 26/01/2023, **Accepted:** 01/03/2023, **Published:** 31/03/2023

Abstract

The adsorption behavior of aluminium ions on chamotte clay has been studied in this study. Chamotte clay has been used for the first time for determination of trace levels of aluminium in aqueous solutions. Quantitative adsorption and recovery of aluminium were both rapid and reached an equilibrium in 30 minutes. Aluminium was detected based on the formation of the highly fluorescent Al(III)-morin complex. Two linear calibration graphs were obtained in the range of 0.5-10 $\mu\text{g L}^{-1}$ and 10-100 $\mu\text{g L}^{-1}$ with the detection limits of 0.12 $\mu\text{g L}^{-1}$ and 1.12 $\mu\text{g L}^{-1}$, respectively. Chamotte clay was characterized by scanning electron microscope coupled with energy-dispersive X-ray spectroscopy, energy dispersive X-ray fluorescence and X-ray photoelectron spectroscopy techniques. Different isotherm models were evaluated and the results showed that the adsorption study was fitted to Freundlich isotherm and a favorable and multilayer adsorption of aluminium was occurred on the heterogeneous surface of the chamotte clay. Thermodynamic and kinetic parameters of aluminium adsorption were also investigated. Various experimental parameters were optimized and the method has been applied to tap and bottled drinking water samples and quantitative recoveries were obtained. The results demonstrated that the chamotte clay, as a natural clay, was expected to be a promising adsorbent for the determination and preconcentration of the trace levels of analyte in real samples.

Keywords: aluminium, separation, clay, adsorption, fluorescence

Şamot Kili: Alüminyumun Ayrılması ve Önderiştirilmesi için Doğal Bir Adsorban

Öz

Bu çalışmada alüminyum iyonlarının şamot kili üzerine olan adsorpsiyon davranışı incelenmiştir. Şamot kili, sulu çözeltilerde eser miktarda alüminyumun tayini için ilk kez kullanılmıştır. Alüminyumun kantitatif adsorpsiyonu ve geri kazanımı hızlı olup 30 dakikada dengeye ulaşmıştır. Alüminyum, floresan özellik gösteren Al(III)-morin kompleksinin oluşumuna dayalı olarak tespit edilmiştir. Çalışmada, 0.5-10 $\mu\text{g L}^{-1}$ ve 10-100 $\mu\text{g L}^{-1}$ aralığında, sırasıyla 0.12 $\mu\text{g L}^{-1}$ ve 1.12 $\mu\text{g L}^{-1}$ belirlenme sınırları ile iki ayrı lineer kalibrasyon grafiği elde edilmiştir. Şamot kili, taramalı elektron mikroskobu-enerji dağılım spektroskopisi, enerji dağılımlı X-ışını floresans ve X-ışını fotoelektron spektroskopisi teknikleri ile karakterize edilmiştir. Farklı izoterm modelleri incelenmiş ve sonuçlar adsorpsiyonun Freundlich izotermine uyduğunu ve şamot kilinin heterojen yüzeyinde alüminyumun çok katmanlı adsorpsiyonunun gerçekleştiğini göstermiştir. Alüminyum adsorpsiyonuna ilişkin termodinamik ve kinetik parametreler de incelenmiştir. Çeşitli deneysel parametreler optimize edilmiş ve yöntem musluk ve şişelenmiş içme suyu numunelerine uygulanmış ve nicel geri kazanımlar elde edilmiştir. Sonuçlar, doğal bir kil olarak şamot kilinin, gerçek örneklerde eser miktarda analitin belirlenmesi ve önderiştirilmesi için umut verici bir adsorban olmasının beklendiğini göstermiştir.

Anahtar Kelimeler: alüminyum, ayırma, kil, adsorpsiyon, floresans

1. Introduction

Aluminium is the most abundant metal and the third most abundant element after oxygen and silicon in the Earth's crust [1,2]. Aluminium has a wide range of applications such as food packaging and drinking materials, electrical wires and metal equipments, construction and machinery [3,4]. The excessive use of aluminium has resulted in contamination of food, environmental or biological samples. Aluminium mainly enters the human body through the consumption of food and water [5] whereas WHO set the tolerable value of aluminium in drinking water to 0.2 mg L^{-1} [6]. Studies over the last decade reveal that aluminium accumulates in internal organs and excessive levels can cause harmful effects to lungs and kidneys [7,8]. Parkinson's and Alzheimer's diseases are also linked to overdose of aluminium in the human body [9-11]. Thus, separation and quantitative determination of trace levels of aluminium in aqueous samples is crucial.

Several instrumental methods including atomic absorption spectrometry (AAS) [12] inductively coupled plasma-mass spectrometry (ICP-MS) [13] and inductively coupled plasma atomic emission spectrometry (ICP-AES) [14] have been used for the determination of aluminium in different types of samples. Aluminium can also be determined by electrochemical [15] and spectroscopic methods such as spectrophotometry [16] and spectrofluorimetry [17].

Fluorimetric sensing systems have been widely used for the determination of different metal ions due to their high sensitivity, selectivity, rapidity and simplicity [18,19]. Highly sensitive fluorimetric analysis of aluminium is mainly based on the formation of fluorescent complexes with different reagents including morin [20,21], lumogallion [22], 8-hydroxyquinoline [23] and different Schiff bases synthesized in the laboratory [24,25]. However, determination of trace levels of analyte in real samples is very difficult due to matrix effects and the lack of detection limits of instruments. Therefore, preconcentration of aluminium before its determination is essential and necessary.

Numerous of organic and inorganic adsorbents have been used for the separation and preconcentration of metal ions [26-29]. Especially over the last decade, natural adsorbents have been widely used in metal ion analysis [30,31]. Among the natural adsorbents, different types of natural clay are attracting attention, for their non-toxicity, stability, low-cost and abundance [32]. Kaolinite [33,34], montmorillonite [35,36], vermiculite [37] and bentonite [38-39] are some of the natural clays which were used as adsorbents for the separation and detection of different metal ions. In the literature, it was reported that chamotte clay was used for the palm kernel biodiesel purification [40] and adsorption of lead(II) [41]. However, to the best of my knowledge, a method based on the usage of chamotte clay for separation, preconcentration and determination of aluminium has not been proposed yet.

This study focuses on the development of a method based on the preconcentration and determination of aluminium using chamotte clay. Chamotte clay was used in this study for the first time for separation and determination of aluminium in aqueous samples. Separation and preconcentration of aluminium with the usage of chamotte clay was combined with spectrofluorimetric detection based on the highly fluorescent aluminium(III)-morin complex

which provides high sensitivity for the detection of aluminium. The adsorbent was characterized using energy dispersive X-ray fluorescence spectroscopy (EDXRF), scanning electron microscopy-energy dispersive X-ray spectroscopy (SEM-EDX) and X-ray photoelectron spectroscopy (XPS). Kinetics and the thermodynamic parameters of the adsorption were also evaluated. Various experimental parameters were optimized and the developed method has been successfully applied to aqueous samples for determination of trace levels of aluminium.

2. Materials and Methods

2.1. Materials

$\text{Al}(\text{NO})_3 \cdot 9\text{H}_2\text{O}$, $\text{FeCl}_2 \cdot 4\text{H}_2\text{O}$, $\text{FeCl}_3 \cdot 6\text{H}_2\text{O}$, HCl, HNO_3 , CH_3COOH , NaOH and absolute ethanol were purchased from Merck (St. Louis, MO, USA). Chamotte clay was obtained from a local company (Desmark, Izmir, Turkey). Morin hydrate were purchased from Fluka (Portland, OR, USA). Ultrapure water was used in all studies (Millipore, Bedford, MA, USA).

1000 mg L^{-1} stock standard solution of aluminium was prepared by dissolving the appropriate amount of $\text{Al}(\text{NO})_3 \cdot 9\text{H}_2\text{O}$ in 10 mL ultrapure water. 100 mg L^{-1} morin solution was prepared by dissolving appropriate amount of morin hydrate in 50 mL absolute ethanol. Working standard solutions were prepared daily by diluting the stock standard solution with ultrapure water. All solutions were stored at 4°C in refrigerator.

2.2. Instrumentation

Fluorimetric determination of aluminium was carried out with a RF-5301 PC spectrofluorometer (Shimadzu, Japan). Energy dispersive X-ray fluorescence (EDXRF) spectrometer was used for determining the elemental composition of chamotte clay (Rigaku, Japan). Apreo S LoVac model scanning electron microscope (SEM) coupled with energy-dispersive X-ray spectroscopy (EDX) was used for determining the morphology and elemental analysis of the adsorbent (Thermoscientific, USA). For SEM analysis, the sample surfaces were coated with gold and the surface was made conductive under vacuum. SEM images were taken at different magnification rates with an acceleration voltage of 20 kV. X-ray photoelectron spectra (XPS) were recorded on a Thermo Scientific K-alpha X-ray photoelectron spectrometer (ThermoFisher, E. Grinstead, UK). A AV264 model balance was used for weight measurements (Ohaus, USA). pH meter was used for measuring and adjusting the pH of the solutions (Hanna Instruments, Woonsocket, RI, USA). All experiments were carried out in a shaking incubator (Wisd Laboratory Instruments, Wertheim, Germany) at a shaking speed of 150 rpm. Sigma 3 - 18 KS model centrifuge was used for the separation of the phases (Sigma, Germany). Visual Minteq program version 3.0 (Stockholm, Sweden) was used for the determination of the dominant chemical form of aluminium.

2.3. Adsorption and recovery procedures for aluminium

For adsorption of aluminium, 5 mL, 1 mg L^{-1} aluminium solution in ultrapure water (with pH values in the range of 2.0-10.0) was added onto 25 mg of chamotte clay. The mixture was

shaken for 30 minutes at 25°C. After adsorption, chamotte clay was separated from the solution by centrifuging at 10,000 rpm for 5 minutes and aluminium in the solution was measured with spectrofluorometer.

For recovery of aluminium, in the first step, adsorption procedure was applied as explained above. HCl, HNO₃ and CH₃COOH with the concentrations of 0.1, 0.5 and 1 mol L⁻¹ were used for determining the quantitative recovery of the analyte. However, unexpectedly high signal was measured in 1 mol L⁻¹ acidic medium, possibly due to the partial dissolution of the clay. 0.1 mol L⁻¹ HCl supplies the highest recovery value and selected as the recovery agent. Thus, after adsorption, separation of chamotte clay was performed and 5 mL, 0.1 mol L⁻¹ HCl was added onto adsorbent and shaken for 30 minutes for recovery of the adsorbed aluminium. Aluminium in the solution was measured with spectrofluorometer.

2.4. Fluorimetric determination of aluminium

Fluorimetric determination of aluminium was based on the formation of the highly fluorescent Al(III)-morin complex. In order to obtain the highly fluorescent compound, firstly, pH of Al(III) solution was adjusted to 3.5 with HCl-NaOH. Then, 0.8 mL of 100 mg L⁻¹ morin solution was added onto 2.5 mL of Al(III) solution and the solution was diluted to 5 mL with absolute ethanol. The emission spectra of the solutions were recorded after 15 minutes in the wavelength range from 440 nm up to 600 nm, using 420 nm as the excitation wavelength and 498 nm as the maximum emission wavelength. Fluorescence spectrum of Al(III)-morin complex is shown in Fig. S1.

3. Results and Discussion

3.1. Characterization of chamotte clay

Chamotte clay was characterized with XPS, SEM-EDX and EDXRF analysis. As shown in the SEM image in Fig. 1, chamotte clay has a porous layered structure with irregular shapes and various sizes. Elemental composition of chamotte clay was determined using XPS, EDXRF and EDX. XPS gives the atomic percentage, EDXRF gives the weight percentage and EDX gives both of the data for the amount of the elements. EDX analysis gathers the chemical information that refers to the surface of the material and may differ from the original bulk composition. However, the similar values were obtained from the analyses and the results are shown in Table 1. Only for XPS analysis, carbon was detected on the surface of the adsorbent which may be due to the atmospheric contamination [42]. According to the results, chamotte clay was mainly composed of Si, Al and O which were attributed to SiO₂ and Al₂O₃ with the trace amounts of Fe, Ca, Ti, Mg, Na and K.

Table 1. Elemental composition of chamotte clay.

Method	Al	Si	O	Fe	Ca	Ti	Mg	Na	K
EDXRF (weight %)	5.1	22.3	70.2	0.8	0.3	0.5	0.2	-	0.7
XPS (atomic %)	12.8	18.5	58.6	0.4	0.4	0.1	0.7	0.3	0.5
EDX (atomic- weight %)	12.3-8.8	26.9-18.5	58.6-70.7	0.7-0.3	0.2-0.1	0.2-0.1	0.8-0.6	0.7-0.6	0.9-0.5

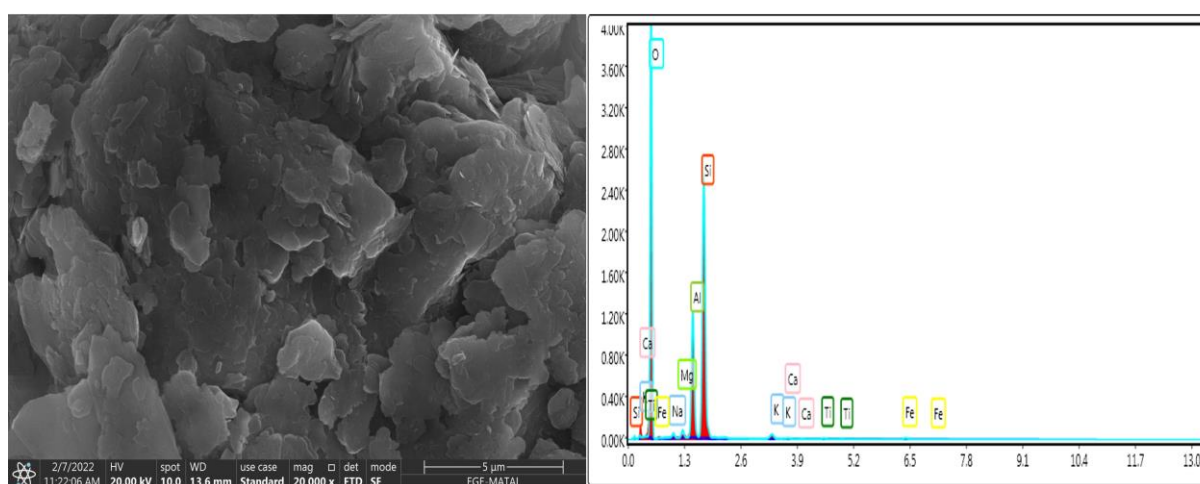


Figure 1. SEM-EDX analysis of chamotte clay (applied voltage: 20 kV, working distance: 13.6 mm, magnification: 20000x).

3.2 Effect of initial pH on the adsorption of Aluminium

The efficiency of aluminium adsorption was affected by the initial pH of the solution as pH not only determines the surface charge of the sorbent but also influences chemical speciation in the solution. In order to investigate the effect of pH on the adsorption efficiency of aluminium, the pH of the water solutions were adjusted in the range of 2.0 to 10.0 using hydrochloric acid (HCl) or sodium hydroxide (NaOH) solutions at various concentrations. As shown in Fig. 2, the maximum adsorption efficiency for Al(III) was observed at pH 7.5. At lower pH values (pH<4, acidic pH values), the adsorption efficiency decreases due to the competitive sorption with proton ions. With increasing pH (4<pH<7), the amount of proton ions decreases which favours the adsorption of aluminium ions. In higher pH values (pH>8), aluminium not only exists in the form of hydroxides which may precipitate depending its concentration but also exists ions with negative charge which cause an electronic repulsion with the adsorbent which has a negative surface charge as stated below. Thus, in alkaline pH values, there is a decrease

in the adsorption efficiency. Using the Visual Minteq software, it was found that the dominant chemical form of aluminium at pH 7.5 is $\text{Al}(\text{OH})_4^-$. Thus, it was concluded that the quantitative adsorption of aluminium at pH 7.5 can be proceeded in the form of $\text{Al}(\text{OH})_4^-$.

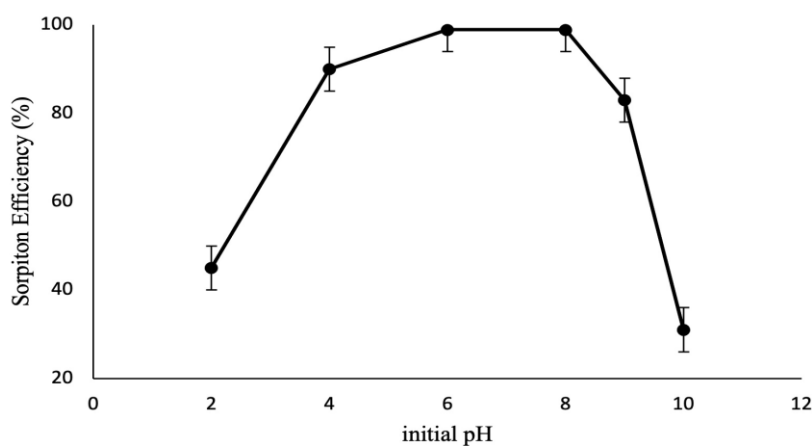


Figure 2. Effect of initial pH on aluminium adsorption (amount of clay: 25 mg, sample volume: 5 mL, initial aluminium(III) concentration: 1 mg L^{-1} , contact time: 30 minutes, pH: 2-10).

The surface charge of the adsorbent was also investigated to identify the sorption mechanism of aluminium. The pH of the point of zero charge (pH_{pzc}) of chamotte clay was determined using the pH drift method [43]. As stated in the literature [44], the point of zero charge (pH_{pzc}) can be defined as the pH of the solution at which charge of the positive surface sites is equal to that of the negative ones, thus, the sorbent surface charge has zero value. The surface charge is negative at $\text{pH} > \text{pH}_{\text{pzc}}$ and positive at $\text{pH} < \text{pH}_{\text{pzc}}$ [45].

For the determination of pH_{pzc} , the pH of a solution of 0.01 M NaCl was adjusted in the range of 2-12 with the addition of either HCl or NaOH. The initial and final pH (after 24 h) values were recorded and the graph of final pH versus initial pH was used to determine the point at which the initial pH and final pH values were equal which was taken as pH_{pzc} . The Fig. S2 shows the pH_{pzc} of the chamotte clay determined with the pH drift method. As shown from the Fig. S2, the pH_{pzc} of the chamotte clay was determined as 7.8. In acidic pH values, both dominant species of aluminium and chamotte clay has a positive charge and in alkaline pH values ($\text{pH} > 8$) both dominant species of aluminium and chamotte clay has a negative charge, for both cases, an electronic repulsion occurs and adsorption efficiency decreases. However, for pH between 7 and 7.8, dominant species of aluminium, $\text{Al}(\text{OH})_4^-$, is negatively charged and chamotte clay is positively charged thus, attractive interaction occurs and adsorption efficiency increases and reaches its maximum. Thus, pH 7.5 was selected as the optimum pH for the determination and preconcentration of trace levels of aluminium.

3.3 Effect of time on adsorption and recovery of aluminium

Contact time is an important parameter that affects the diffusion of metal ions onto adsorbent which determines the sorption/removal efficiency and recovery values.

Fig. 3 shows the effect of time on adsorption and recovery of aluminium. According to Fig. 3, quantitative adsorption and recovery of aluminium were both rapid and reached an equilibrium in 30 minutes. It can be concluded that the rapid adsorption was observed due to the abundant availability of the active sites on the surface of the chamotte clay.

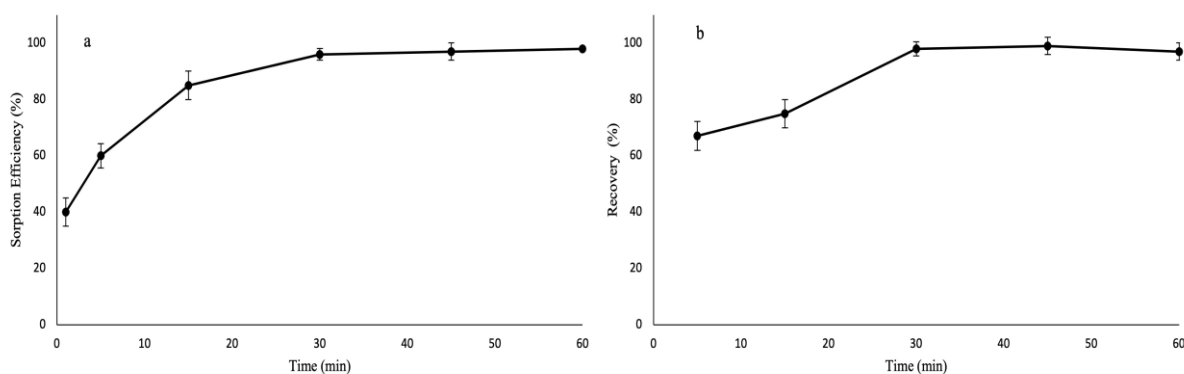


Figure 3. Effect of time on a) adsorption and b) recovery (amount of clay: 25 mg, sample volume: 5 mL, time: 0-60 minutes).

3.4 Effect of adsorbent dosage

In order to ensure the quantitative adsorption of aluminium in different sample volumes, usage of the minimum adsorbent dosage is very important. As shown in Fig. 4, 5 g L^{-1} is the required adsorbent dosage for the quantitative adsorption of aluminium. It can be concluded that the number of active sites increases as the amount of clay increases up to 5 g L^{-1} which supplies an increase in the adsorption efficiency. Increasing the adsorbent dosage had no effect on adsorption efficiency above 5 g L^{-1} and in order to use the minimum amount of sorbent and provide more economical method 5 g L^{-1} was used in the study.

Table 2. Isotherm models for aluminium adsorption.

Adsorption model	Equation	Parameters of the Equation
Freundlich	$\ln q_e = \ln K_F + \frac{1}{n} \ln C_e$	$K_F = 0.53 \text{ mg g}^{-1}$ $n = 2.64$ $R^2 = 0.9917$
Langmuir	$\frac{C_e}{q_e} = \frac{1}{K_L Q_m} + \frac{C_e}{Q_m}$	$Q_m = 2.66 \text{ mg g}^{-1}$ $K_L = 0.13 \text{ L mg}^{-1}$ $R^2 = 0.9323$
Dubinin–Radushkevich	$\ln q_e = \ln q_m - k\varepsilon^2$ $\varepsilon = (2k)^{-0.5}$	$k = 0.018 \text{ mol}^2 \text{ kJ}^{-2}$ $q_m = 0.00036 \text{ mol g}^{-1}$ $E = 5.24 \text{ kJ mol}^{-1}$ $R^2 = 0.9577$

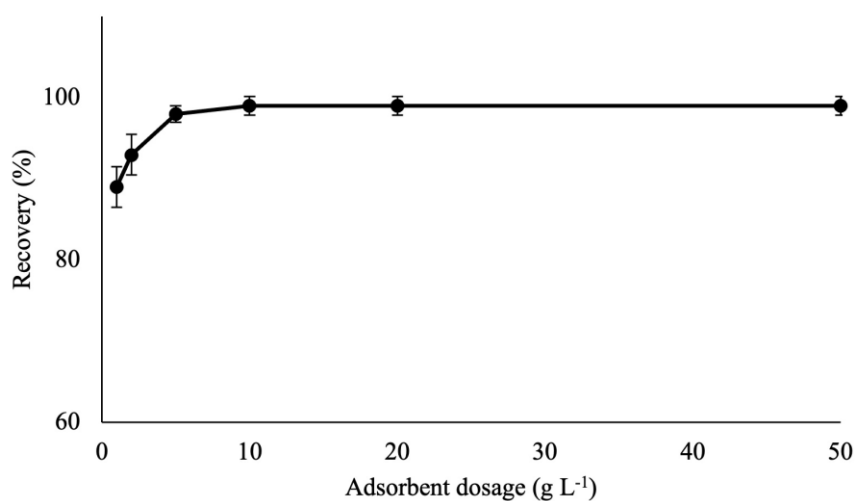


Figure 4. Effect of adsorbent dose (amount of clay: 5-250 mg, sample volume: 5 mL, contact time: 30 minutes, pH: 7.5).

3.5 Sorption isotherm models

The type of the adsorption was determined using Freundlich, Langmuir and Dubinin–Radushkevich (D-R) isotherm models. In order to determine the type of the interaction of the adsorbents with the adsorbate; 10 mg chamotte clay was shaken with 5 mL of various initial concentration of aluminium solution (1-50 mg L⁻¹) in ultrapure water (pH~7.5) for 24 hours. After sorption, clay was separated from the solution with the aid of centrifugation and the amount of aluminium in the solution was determined with spectrofluorometer.

The equations of the isotherm models can be seen at Table 2. In Freundlich isotherm model, q_e is the amount of aluminium adsorbed by the clay (mg g⁻¹), C_e is the equilibrium concentration of aluminium (mg L⁻¹), K_F (mg g⁻¹) and n (dimensionless) are Freundlich constants related to the adsorption capacity and intensity of adsorption, respectively. Freundlich isotherm was obtained by plotting $\ln C_e$ versus $\ln q_e$.

In Langmuir isotherm model, C_e is the equilibrium concentration of aluminium (mg L⁻¹), q_e is the adsorption capacity adsorbed at equilibrium (mg g⁻¹), Q_m is maximum adsorption capacity (mg g⁻¹) and K_L is the Langmuir adsorption constant (L mg⁻¹). Langmuir isotherm was obtained by plotting C_e/q_e versus C_e .

For D-R isotherm model, q_e is the amount of aluminium adsorbed by the clay (mg g⁻¹), q_m is the maximum sorption capacity (mol g⁻¹), k is the activity coefficient related to sorption energy, R is the gas constant (J mol⁻¹K⁻¹), T is the temperature (K), ϵ is the Polanyi potential (mol² J⁻²), C_e is the equilibrium concentration of aluminium (mol L⁻¹) and E is the sorption energy represents the energy required for moving one mole of the solute from infinity to the surface of the adsorbent (kJ mol⁻¹). D-R isotherm was obtained by plotting $\ln q_e$ versus ϵ^2 .

Parameters of the equations were calculated using the slope and intercept of the plots and the results are shown in Table 2. The most suitable isotherm is determined by the correlation coefficient (R^2). The R^2 value closest to 1 indicates the best fit model.

Among the isotherm models, Freundlich isotherm is commonly used to describe the multilayer adsorption and adsorption on heterogeneous surfaces [46-48] whereas Langmuir isotherm represents a monolayer adsorption at specific homogenous sites [49-50]. On the other hand, D-R isotherm both assumes that the adsorption is multilayered and depends on a pore-filling mechanism [51-52]. Considering the correlation coefficients, it can be seen that the sorption process fits to Freundlich isotherm very well. A value of 2.64 obtained for n with the Freundlich isotherm represents that the adsorption is favorable, as it is greater than 1 [53]. Thus, it can be concluded that a favorable and multilayer adsorption of aluminium was occurred on the heterogeneous surface of the chamotte clay.

3.6 Kinetic of aluminium adsorption

10 mL of 5 mg L⁻¹ aluminium solution (pH 7.5) was shaken with 200 mg chamotte clay for different periods of time (from 5 to 1440 min) at 25°C using shaking incubator in order to determine the kinetic parameters of aluminium adsorption. After sorption, clay was separated from the solution using centrifugation and the amount of aluminium in the solution was determined with spectrofluorometer.

The linear pseudo-first-order, pseudo-second-order kinetic and intra-particle diffusion models were applied using the following equations [54,55]:

where q_e is the amount of aluminium adsorbed ($\mu\text{g g}^{-1}$) at equilibrium, q_t is the amount of aluminium adsorbed ($\mu\text{g g}^{-1}$) at time t , k_1 , k_2 and k_{id} are the pseudo-first-order rate constant (min^{-1}), pseudo-second-order rate constant ($\text{g } \mu\text{g}^{-1} \text{ min}^{-1}$) and the intraparticle diffusion rate constant ($\mu\text{g g}^{-1} \text{ min}^{-1/2}$), respectively, t is the time (min) and C ($\mu\text{g g}^{-1}$) represents the boundary layer thickness. Kinetic parameters for the adsorption of aluminium can be shown in Table 3. As shown in Table 3, considering the correlation coefficients, pseudo-second-order model is more suitable to describe the adsorption of aluminium onto chamotte clay. As the adsorption of aluminium fits to pseudo second-order kinetic reaction model, it can be concluded that the chemisorption is the rate-limiting mechanism through sharing or exchange of electrons between adsorbent and adsorbate [56].

$$\log(q_e - q_t) = \log q_e - \frac{k_1}{2.303} t \quad (1)$$

$$\frac{t}{q_t} = \frac{1}{k_2 q_e^2} + \frac{t}{q_e} \quad (2)$$

$$q_t = k_{id} t^{\frac{1}{2}} + C \quad (3)$$

Table 3. Kinetic parameters of different models for the sorption of aluminium.

Kinetic model	Parameters
pseudo-first-order	$q_e = 64.18 \mu\text{g g}^{-1}$ $k_1 = 0.004 \text{ min}^{-1}$ $R^2 = 0.4704$
pseudo-second-order	$q_e = 43.5 \mu\text{g g}^{-1}$ $k_2 = 0.025 \text{ g } \mu\text{g}^{-1} \text{ min}^{-1}$ $R^2 = 0.9996$
intra-particle diffusion	$C = 40.47 \mu\text{g g}^{-1}$ $k_{id} = 0.1995 \mu\text{g g}^{-1} \text{ min}^{-1/2}$ $R^2 = 0.9764$

3.7 Thermodynamics of aluminium adsorption

In order to determine the thermodynamic parameters of the aluminium adsorption, experiments were carried out at three different temperatures. 10 mL of 5 mg L⁻¹ aluminium solution (pH 7.5) was shaken with 200 mg chamotte clay for 30 minutes at 25°C, 35°C and 45°C using temperature controlled shaking incubator. After sorption, chamotte clay was separated from the solution using centrifugation and the amount of aluminium in the solution was determined with spectrofluorometer. Gibbs free energy change (ΔG^0), enthalpy (ΔH^0) and entropy (ΔS^0) were calculated from the following equations [57-58]:

$$\Delta G^0 = -RT \ln K_C, \quad K_C = \frac{C_s}{C_e} \quad (4)$$

$$\ln K_C = \frac{\Delta S^0}{R} - \frac{\Delta H^0}{RT} \quad (5)$$

$$\Delta G^0 = \Delta H^0 - T\Delta S^0 \quad (6)$$

where K_C is the equilibrium constant, C_s is the amount of analyte adsorbed by adsorbent (mg g⁻¹), C_e is the equilibrium concentration of aluminium (mg L⁻¹), R is the gas constant (8.314 J mol⁻¹ K⁻¹) and T is the temperature (K). Parameters change in enthalpy (ΔH^0) and change in entropy (ΔS^0) were calculated from the slope and the intercept of the linear plot of $\ln K_C$ versus $1/T$. The calculated thermodynamic parameters are summarized in Table 4.

As mentioned in the literature, ΔG value lower than 20 kJ mol^{-1} states physical adsorption while values above 40 kJ mol^{-1} indicates the chemical adsorption and the negative values indicate the spontaneous nature of the sorption [59]. Negative ΔH^0 values emphasize that the adsorption is exothermic and the adsorption capacity decreases with an increase in the temperature [60]. If the value of ΔH^0 is lower than 40 kJ mol^{-1} the adsorption process is physisorption while the value is more than 100 kJ mol^{-1} the type of adsorption is chemisorption [61]. A negative ΔS^0 value denotes the decreased randomness at the solid–solution interface during the adsorption process [62]. When the thermodynamic parameters evaluated, it is evaluated that the aluminium adsorption is exothermic due to the negative value of ΔH^0 , spontaneous and favorable due to the negative value of ΔG^0 and the degree of freedom decreased at the liquid-solid interface due to the negative value of ΔS^0 .

Table 4. Thermodynamic parameters for aluminium adsorption.

Temperature (K)	ΔG^0 (kJ mol ⁻¹)	ΔH^0 (kJ mol ⁻¹)	ΔS^0 (kJ mol ⁻¹ K ⁻¹)
298	-6.73	-16.13	-0.03
308	-6.42		
318	-6.10		

3.8 Analytical figures of merit

The aluminium content in the solution was determined via the formation of the highly fluorescent aluminium(III)-morin complex in acidic medium. As stated in the literature [21], the addition of ethanol into aqueous system increases the fluorescence signal of the complex. Two calibration graphs were obtained for two different range of aluminium. Using a slit width of 5 nm, the calibration graph (calibration graph #1) was linear within the range of $0.5\text{-}10 \mu\text{g L}^{-1}$ with an equation of $y = 82993x + 149625$ and a correlation coefficient (R^2) of 0.9991 ($n=3$). When the slit width set to 3 nm, the calibration graph (calibration graph #2) was linear within the range of $10\text{-}100 \mu\text{g L}^{-1}$ with an equation of $y = 9777.5x + 33040$ and a correlation coefficient (R^2) of 0.9971 ($n=3$).

Limit of detection (LOD) and limit of quantification (LOQ) were calculated using the equations;

$$LOD = \frac{\sigma}{S} \times 3 \quad (7)$$

and

$$LOQ = \frac{\sigma}{S} \times 10 \quad (8)$$

where σ is the standard deviation of the responses of the blank solution and S is the slope of the calibration curve [63,64].

For the calibration graph #1, LOD and LOQ were calculated as $0.12 \mu\text{g L}^{-1}$ and $0.39 \mu\text{g L}^{-1}$, respectively, whereas LOD and LOQ were calculated as $1.18 \mu\text{g L}^{-1}$ and $3.95 \mu\text{g L}^{-1}$, respectively, for the calibration graph #2.

In order to determine the precision of the method, relative standard deviations (RSDs) of intra-day and inter-day precisions of three different concentration levels of aluminium were determined for the obtained calibration graphs. $2.5, 5.0$ and $7.5 \mu\text{g L}^{-1}$ aluminium(III) solutions were used for the precision study for calibration graph #1 where $25, 50$ and $75 \mu\text{g L}^{-1}$ aluminium(III) solutions were used for the precision study for calibration graph #2. The intra-day precision was determined with the five repeated measurements of the samples on the same day and the inter-day precision was determined by measuring the sample once a day for five consecutive days. RSD values of intra-day and inter-day studies were found to be in the range of $0.8 - 1.4 \%$ and $1.2 - 1.5 \%$ for calibration graph #1 and $1.2 - 1.8 \%$ and $1.5 - 2.2 \%$ for calibration graph #2, respectively.

Table 5 summarizes a comparison of the general performance parameters for the published methods used for the determination and preconcentration of aluminium. When the parameters were compared, the developed method based on the preconcentration of aluminium using chamotte clay was expected to be a promising method for the determination and preconcentration of the trace levels of analyte in real samples.

Table 5. Comparison of the analytical performance of published methods with the present work for the determination of aluminium.

Working range	Limit Detection	of	Method	Reference
1–50 $\mu\text{g L}^{-1}$	1.7 $\mu\text{g L}^{-1}$		fabric phase sorptive extraction-high performance liquid chromatography-UV detection	[65]
5-1600 $\mu\text{g L}^{-1}$	1.5 $\mu\text{g L}^{-1}$		graphene oxide modified (4-phenyl) methanethiol nanomagnetic composite-atom trap flame atomic absorption spectrometer	[11]
-	0.2 $\mu\text{g L}^{-1}$		8-hydroxyquinoline–cobalt(II) coprecipitation system-UV–vis spectrophotometry	[66]
27 $\mu\text{g L}^{-1}$ - 270 mg L^{-1}	6.6 $\mu\text{g L}^{-1}$		all-solid-state potentiometric detection	[8]
0.5-10 $\mu\text{g L}^{-1}$ and 10-100 $\mu\text{g L}^{-1}$	0.12 $\mu\text{g L}^{-1}$ and 1.12 $\mu\text{g L}^{-1}$		chamotte clay-fluorescence detection	This study

3.9 Reusability of the adsorbent

Reusability of the same chamotte clay was investigated since the reusability of the same adsorbent affects the cost of the developed method. Ten cycles of sorption-recovery procedures were applied to the same adsorbent and according to the recovery values 98.9 ± 1.3 ($n=10$), it was observed that same adsorbent can be used for ten times for the determination of aluminium.

3.10 Interference effects

The interference effects of other cations, such as Na(I), K(I), Mg(II), Ca(II), Co(II), Fe(II), Fe(III), Mn(II), Co(II), Ni(II), Zn(II), Cd(II), and Pb(II) and anions such as chloride, nitrate, sulphate and phosphate on the recovery of aluminium(III) were investigated. The interference effect was studied independently for each of the ions. 5 mL of $10 \mu\text{g L}^{-1}$ aluminium solution

(pH 7.5) with different concentrations of ions was shaken with 25 mg chamotte clay for 30 minutes. After sorption, chamotte clay was separated from the solution using centrifugation and 5 mL 0.1 M HCl was added onto adsorbent and shaken for 30 minutes for recovery of aluminium. Then, the fluorimetric determination procedure was applied. The tolerable ratios of all investigated ions were investigated up to 1 mg L⁻¹ (100-fold) and it was found that the investigated ions did not exhibit any remarkable change (> ±5%) on the recovery of aluminium.

3.11 Analytical application

The developed method was applied to both tap and bottled drinking water samples. Before the analysis, water samples were first filtered through a filter paper. After adjusting the pH values to 7.5, 50 mL of water samples were shaken with 250 mg chamotte clay for 30 minutes for the adsorption of aluminium. After sorption of aluminium, chamotte clay was separated from the solution with centrifugation. 5.0 mL 0.1 M HCl was added onto chamotte clay and shaken for 30 minutes for the recovery of aluminium. After centrifugation, the phases were separated and the pH of the solution was adjusted to 3.5. Then, 0.8 mL of 100 mg L⁻¹ morin solution was added onto 2.5 mL of the solution and the solution was diluted to 5 mL with absolute ethanol. The preconcentration factor for both analyses was 10. The amount of aluminium in the solution was measured with spectrofluorometer ($\lambda_{\text{ex}}=420$ nm and $\lambda_{\text{em}}=498$ nm). Spike addition was also applied to the samples and the results of the sample applications are shown in Table 6. The quantitative recovery values revealed that the developed method can be applied to aqueous samples for the determination of aluminium.

Table 6. Sample application of the method.

Sample	Added ($\mu\text{g L}^{-1}$)*	Found ($\mu\text{g L}^{-1}$)*	Recovery (%)
Tap water	-	0.39±0.07	-
	10	10.68±0.18	102.82±1.69
	25	25.40±0.56	100.04±2.19
	50	50.87±0.61	100.95±1.21
Bottled drinking water	-	<LOD**	-
	10	9.83±0.25	98.33±2.52
	25	25.03±0.32	100.13±1.29
	50	49.83±1.27	99.67±2.53

*(n=3)

**LOD = Limit of Detection

4. Conclusion

The present work involves the development of a method for determination of aluminium in aqueous samples based on the usage of chamotte clay. Chamotte clay has been used for the first time for determination of trace levels of aluminium. Quantitative adsorption and recovery of aluminium were both rapid and reached an equilibrium in 30 minutes. The adsorption study was fitted to Freundlich isotherm and multilayer adsorption of aluminium was occurred on the heterogeneous surface of the chamotte clay. Thermodynamic parameters revealed that the aluminium adsorption is exothermic, spontaneous and favorable. The method is applied to tap and bottled drinking water samples and the recoveries were found to be in the range of 98.3 and 102.8 %. The preconcentration factor of both analyses was determined as 10 and same adsorbent can be used for ten times for the determination of aluminium. Upon the evaluation of the analytical parameters, the developed method was expected to be a promising method for the determination and preconcentration of the trace levels of analyte in real samples.

Acknowledgment

The author would like to thank Dr. Ece Bayır for her great support and valuable comments on this paper.

Ethics in Publishing

There are no ethical issues regarding the publication of this study.

References

- [1]. Arunakumara, K. K. I. U. Walpola, B. C. Yoon, M. H. (2013) Aluminum toxicity and tolerance mechanism in cereals and legumes – a review. *J. Korean Soc. Appl. Biol. Chem.*, 56, 1–9.
- [2]. Sidqi, M. E. Aziz, A. A. A. Abolehasan, A. E. Sayed, M. A. (2022) Photochemical processing potential of a novel Schiff base as a fluorescent probe for selective monitoring of Al³⁺ ions and bioimaging in human cervical cancer HeLa cells. *J. Photochem. Photobiol.*, 424, 113616.
- [3]. Gupta, V. K. Shoor, S. K. Kumawat, L. K. Jain, A. K. (2015) A highly selective colorimetric and turn-on fluorescent chemosensor based on 1-(2-pyridylazo)-2-naphthol for the detection of aluminium(III) ions. *Sens. Actuators B Chem.*, 209, 15-24.
- [4]. Abbaspour, A. Refahi, M. Khalafinezhad, A. Rad, M. N. S. Behrouz, S. (2010) A selective and sensitive carbon composite coated platinum electrode for aluminium determination in pharmaceutical and mineral water samples. *Anal. Chim. Acta.*, 662, 76–81.
- [5]. Loeschner, K. Correia, M. Chaves, C. L. Rokkjær, I. Sloth, J. J. (2018) Detection and characterisation of aluminium-containing nanoparticles in Chinese noodles by single particle ICP-MS. *Food Addit. Contam. Part A.*, 35, 6-93.

- [6]. WHO, (2011) Aluminium, guidelines for drinking water quality. 4th ed., World Health Organization, Geneva.
- [7]. Kejík, Z. Kapláne, R. Havlík, M. Bříza, T. Vavřinová, D. Dolenský, B. Martásek, P. Král, V. (2016) Aluminium(III) sensing by pyridoxal hydrazone utilising the chelation enhanced fluorescence effect. *J. Lumin.*, 180, 269-277.
- [8]. Ying, K. S. Heng, L. Y. Hassan, N. I. Hasbullah, S. A. (2020) A new and all-solid-state potentiometric aluminium ion sensor for water analysis. *Sensors.*, 20, 6898.
- [9]. Suherman, A. L. Tanner, E. E. L. Kuss, S. Sokolov, S. V. Holter, J. Young, N. P. Compton, R. G. (2018) Voltammetric determination of aluminium(III) at tannic acidcapped-gold nanoparticle modified electrodes. *Sens. Actuators B Chem.*, 265, 682-690.
- [10]. Youssef, H. M. Azzam, M. A. (2021) Efficient removal of aluminium(III) from aqueous solutions via ion-flotation technique using aluminon as a chelating agent and oleic acid as a surfactant. *Int. J. Environ. Anal. Chem.*, 1-18.
- [11]. Shirkhanloo, H. Abbasabadi, M. K. Hosseini, F. Zarandi, A. F. (2021) Nanographene oxide modified phenyl methanethiol nanomagnetic composite for rapid separation of aluminum in wastewaters, foods, and vegetable samples by microwave dispersive magnetic micro solid-phase extraction. *Food Chem.*, 347, 129042.
- [12]. Komarek, J. Cervenka, R. Ruzicka, T. Kuban, T. (2007) ET-AAS determination of aluminium in dialysis concentrates after continuous flow solvent extraction. *J. Pharmaceut. Biomed.*, 45, 504-509.
- [13]. Eroglu, E. I. Gulec, A. Ayaz, A. (2018) Determination of aluminium leaching into various baked meats with different types of foils by ICP-MS. *J. Food Process. Preserv.*, 42, e13771.
- [14]. Samarina, T. O. Volkov, D. S. Mikheev, I. V. Proskurnin, M. A. (2018) High-sensitivity and high-performance determination of trace aluminum in water for pharmaceutical purposes by microwave plasma and inductively coupled plasma-atomic emission spectrometry. *Anal. Lett.*, 51, 659-672.
- [15]. Thomas, S. D. Davey, D. E. Mulcahy, D. E. Chow, C. W. K. (2005) Indirect amperometric detection of aluminium by flow injection analysis using DASA as ligand. *Anal. Lett.*, 38, 133-147.
- [16]. Elečková, L. Alexovič, M. Kuchár, J. Balogh, I. S. Andruch, V. (2015) Visual detection and sequential injection determination of aluminium using acinnamoyl derivative. *Talanta.*, 133, 27-33.
- [17]. Anwar, Z. M. Ibrahim, I. A. Kamel, R. M. Salam, E. T. A. Asfoury, M. H. E. (2018) New highly sensitive and selective fluorescent terbium complex for the detection of aluminium ions. *J. Mol. Struct.*, 1154, 272-279.
- [18]. Kamel, R. M. Sakka, S. S. E. Bahgat, K. Monir, M. R. Soliman, M. H. A. (2021) New turn on fluorimetric sensor for direct detection of ultra-trace ferric ions in industrial wastewater and its application by test strips. *J. Photochem. Photobiol.*, 411, 113218.
- [19]. Pomal, N. C. Bhatt, K. D. Modi, K. M. Desai, A. L. Patel, N. P. Kongor, A. Kolivoška, V. (2021) Functionalized silver nanoparticles as colorimetric and fluorimetric sensor for environmentally toxic mercury ions: an overview. *J. Fluoresc.*, 31, 635-649.

- [20]. Renedo, O. D. Cuñado, A. M. N. Romaya, E. V. Lomillo, M. A. A. (2019) Determination of aluminium using different techniques based on the Al(III)-morin complex. *Talanta.*, 196, 131-136.
- [21]. Mateos, A. A. Parra, M. J. A. Serrano, Y. C. Martín, F. J. R. (2008) Online monitoring of aluminium in drinking water with fluorimetric detection. *J. Fluoresc.*, 18, 183-192.
- [22]. Chu, F. Han, P. Feng, S. Wei, S. Ma, H. Bian, Z. (2021) Hydrogel optical fibers functionalized with lumogallion as aluminum ions sensing platform. *Optik.*, 240, 166875.
- [23]. Yamaguchi, S. Matusi, K. (2016) Formation and entrapment of tris(8-hydroxyquinoline)aluminum from 8-hydroxyquinoline in anodic porous alumina. *Materials.*, 9, 715.
- [24]. Peng, H. Han, Y. Lin, N. Liu, H. (2019) Two pyridine-derived Schiff-bases as turn-on fluorescent sensor for detection of aluminium ion. *Opt. Mater.*, 95, 109210.
- [25]. Samanta, S. Nath, B. Baruah, J. B. (2012) Hydrolytically stable Schiff base as highly sensitive aluminium sensor. *Inorg. Chem. Commun.*, 22, 98-100.
- [26]. Kayan, A. (2019) Inorganic-organic hybrid materials and their adsorbent properties. *Adv. Compos. Mater.*, 2, 34-45.
- [27]. Saltan, F. Saltan, G. M. (2022) Synthesis of a new adsorbent poly(allylisothiocyanate-co- hydroxyethylmethacrylate-co-vinylimidazole) via photopolymerization: Characterization and investigation of heavy metal adsorption capacity. *J. Appl. Polym. Sci.*, 139, e52639.
- [28]. Karimi, F. Ayati, A. Tanhaei, B. Sanati, A. L. Afshar, S. Kardan, A. Dabirifar, Z. Karaman, C. (2022) Removal of metal ions using a new magnetic chitosan nano-bio-adsorbent; A powerful approach in water treatment. *Environ. Res.*, 203, 111753.
- [29]. Usman, M. Ahmed, A. Yu, B. Wang, S. Shen, Y. Cong, H. (2021) Simultaneous adsorption of heavy metals and organic dyes by β -cyclodextrin-chitosan based cross-linked adsorbent. *Carbohydr. Polym.*, 255, 117486.
- [30]. Chakraborty, R. Asthana, A. Singh, A. K. Jain, B. Susan, A. B. H. (2022) Adsorption of heavy metal ions by various low-cost adsorbents: a review. *Int. J. Environ. Anal. Chem.*, 102, 342-379.
- [31]. Sdiri, A. T. Higashi, T. Jamoussi, F. (2014) Adsorption of copper and zinc onto natural clay in single and binary systems. *Int. J. Environ. Sci. Technol.*, 11, 1081-1092.
- [32]. Gu, S. Kang, X. Wang, L. Lichtfouse, E. Wang, C. (2019) Clay mineral adsorbents for heavy metal removal from wastewater: a review. *Environ. Chem. Lett.*, 17, 629-654.
- [33]. Doi, A. Khosravi, M. Ejtemaei, M. Nguyen, T. A. H. Nguyen, A. V. (2020) Specificity and affinity of multivalent ions adsorption to kaolinite surface. *Appl. Clay Sci.*, 190, 105557.
- [34]. Fijałkowska, G. Wiśniewska, M. Karpisz, K. S. (2020) Adsorption and electrokinetic studies in kaolinite/anionic polyacrylamide/chromate ions system. *Colloids Surf. A Physicochem. Eng. Asp.*, 603, 125232.

- [35]. Ijagbemi, C. O. Baek, M. H. Kim, D. S. (2009) Montmorillonite surface properties and sorption characteristics for heavy metal removal from aqueous solutions. *J. Hazard. Mater.*, 1, 538-546.
- [36]. Akpomie, K. G. Dawodu, F. A. (2016) Acid-modified montmorillonite for sorption of heavy metals from automobile effluent. *Beni-Seuf Univ. J. Appl.*, 1, 1-16.
- [37]. Brião, G. D. V. Silva, M. G. C. D. Vieira, M. G. A. (2021) Efficient and selective adsorption of neodymium on expanded vermiculite. *Ind. Eng. Chem. Res.*, 60, 4962-4974.
- [38]. Manohar, D. M. Noeline, B. F. Anirudhan, T. S. (2006) Adsorption performance of Al-pillared bentonite clay for the removal of cobalt(II) from aqueous phase. *Appl. Clay Sci.*, 31, 194-206.
- [39]. Bertagnolli, C. Kleinübing, S. J. Silva, M. G. C. D. (2011) Preparation and characterization of a Brazilian bentonite clay for removal of copper in porous beds. *Appl. Clay Sci.*, 53, 73-79.
- [40]. Santos, F. D. Conceição, L. R. V. D. Ceron, A. Castro, H. F. D. (2017) Chamotte clay as potential low cost adsorbent to be used in the palm kernel biodiesel purification. *Appl. Clay Sci.*, 149, 41-50.
- [41]. Rakhym, A. B. Seilkhanova, G. A. Kurmanbayeva, T. S. (2020) Adsorption of lead (II) ions from water solutions with natural zeolite and chamotte clay. *Mater. Today: Proc.*, 31, 482-485.
- [42]. Nita, C. Fullenwarth, J. Monconduit, L. Meins, J. M. L. Fioux, P. Parmentier, J. Ghimbeu, C. M. (2019) Eco-friendly synthesis of SiO₂ nanoparticles confined in hard carbon: a promising material with unexpected mechanism for Li-ion batteries. *Carbon.*, 143, 598-609.
- [43]. Zhang, Z. Moghaddam, L. O'Hara, I. M. Doherty, W. O. S. (2011) Congo red adsorption by ball-milled sugarcane bagasse. *Chem. Eng. J.*, 178, 122-128.
- [44]. Fiol, N. Villaescusa, I. 2009. Determination of sorbent point zero charge: usefulness in sorption studies. *Environ. Chem. Lett.*, 7, 79-84.
- [45]. Kragović, M. Stojmenović, M. Petrović, J. Loredó, J. Pašalić, S. Nedeljković, A. Ristović, I. (2019) Influence of alginate encapsulation on point of zero charge (pHpzc) and thermodynamic properties of the natural and Fe(III) - modified zeolite. *Procedia Manuf.*, 32, 286-293.
- [46]. Syafiqah, M. S. I. Yussof, H. W. (2018) Kinetics, isotherms, and thermodynamic studies on the adsorption of mercury (II) ion from aqueous solution using modified palm oil fuel ash. *Mater. Today Proc.*, 5, 21690-21697.
- [47]. Ayawei, N. Ebelegi, A. N. Wankasi, D. (2017) Modelling and interpretation of adsorption isotherms. *J. Chem.*, 1-11.
- [48]. Wang, J. Liu, G. Li, T. Zhou, C. (2015) Physicochemical studies toward the removal of Zn(II) and Pb(II) ions through adsorption on montmorillonite-supported zero-valent iron nanoparticles. *RSC Adv.*, 5, 29859-29871.
- [49]. Gai, W. Z. Deng, Z. Y. Shi, Y. (2015) Fluoride removal from water using high-activity aluminum hydroxide prepared by the ultrasonic method. *RSC Adv.*, 5, 84223-84231.

- [50]. Rajahmundry, G. K. Garlapati, C. Kumar, P. S. Alwi, R. S. Vod, D. V. N. (2021) Statistical analysis of adsorption isotherm models and its appropriate selection. *Chemosphere.*, 276, 130176.
- [51]. Nnaji, C. C. Agim, A. E. Mama, C. N. Emenike, P. G. C. Ogarekpe, N. M. (2021) Equilibrium and thermodynamic investigation of biosorption of nickel from water by activated carbon made from palm kernel chaff. *Sci. Rep.*, 11, 7808.
- [52]. Roby, R. B. Gagnon, J. Deschênes, J. S. Chabot, B. (2018) Development and treatment procedure of arsenic-contaminated water using a new and green chitosan sorbent: kinetic, isotherm, thermodynamic and dynamic studies. *Pure Appl. Chem.*, 90, 63-77.
- [53]. Hameed, B. M. (2009) Spent tea leaves: a new non-conventional and low-cost adsorbent for removal of basic dye from aqueous solutions. *J. Hazard. Mater.*, 161, 753-759.
- [54]. Fei, F. Gao, Z. Wu, H. Wurendaodi, W. Zhao, S. Asuha, S. (2020) Facile solid-state synthesis of Fe₃O₄/kaolinite nanocomposites for enhanced dye adsorption. *J. Solid State Chem.*, 291, 121655.
- [55]. Kassimi, A. E. Achour, Y. Himri, M. E. Laamari, M. Haddad, M. E. (2021) High efficiency of natural safiot clay to remove industrial dyes from aqueous media: kinetic, isotherm adsorption and thermodynamic studies. *Biointerface Res. Appl. Chem.*, 11, 12717-12731.
- [56]. Shafey, E. S. I. E. Lawati, H. A. Sumri, A. S. A. (2012) Ciprofloxacin adsorption from aqueous solution onto chemically prepared carbon from date palm leaflets. *J. Environ. Sci.*, 24, 1579-1586.
- [57]. Alorabi, A. Q. Hassan, M. S. Alam, M. M. Zabin, S. A. Alsenani, N. I. Baghdadi, N. E. (2021) Natural clay as a low-cost adsorbent for crystal violet dye removal and antimicrobial activity. *Nanomaterial.*, 11, 2789.
- [58]. Okorie, H. O. C. Ekemezie, P. N. Akpomie, K. G. Olikagu, C. S. (2018) Calcined corncob-kaolinite combo as new sorbent for sequestration of toxic metal ions from polluted aqua media and desorption. *Front. Chem.*, 6, 273.
- [59]. Akinbulumo, O. A. Odejebi, O. J. Odekanle, E. L. (2020) Thermodynamics and adsorption study of the corrosion inhibition of mild steel by Euphorbia heterophylla L. extract in 1.5 M HCl. *Results Mat.*, 5, 10074.
- [60]. Ramesh, A. Lee, D. J. Wong, J. W. C. (2005) Thermodynamic parameters for adsorption equilibrium of heavy metals and dyes from wastewater with low-cost adsorbents. *J. Colloid Interface Sci.*, 291, 588-592.
- [61]. Shukla, S. K. Ebenso, E. E. (2011) Corrosion inhibition, adsorption behavior and thermodynamic properties of streptomycin on mild steel in hydrochloric acid medium. *Int. J. Electrochem. Sci.*, 6, 3277-3291.
- [62]. Sahmoune, M. N. (2019) Evaluation of thermodynamic parameters for adsorption of heavy metals by green adsorbents. *Environ. Chem. Lett.*, 17, 697-704.
- [63]. Chen, L. Liu, J. Zeng, Q. Wang, H. Yu, A. Zhang, H. Ding, L. (2009) Preparation of magnetic molecularly imprinted polymer for the separation of tetracycline antibiotics from egg and tissue samples. *J. Chromatogr. A.*, 1216, 3710-3719.

- [64]. Wang, J. Pan, J. Yin, Y. Wu, R. Dai, X. Dai, J. Gao, L. Ou, H. (2015) Thermo-responsive and magnetic molecularly imprinted Fe₃O₄@ carbon nanospheres for selective adsorption and controlled release of 2,4,5-trichlorophenol. *J. Ind. Eng. Chem.*, 25, 321–328.
- [65]. Rekhi, H. Kaur, R. Rani, S. Malik, A. K. Kabir, A. K. G. (2018) Direct rapid determination of trace aluminum in various water samples with quercetin by reverse phase high-performance liquid chromatography based on fabric phase sorptive extraction technique. *J. Chromatogr. Sci.*, 56, 452-460.
- [66]. Bulut, V. N. Arslan, D. Ozdes, D. Soylak, M. Tufekci, M. (2010) Preconcentration, separation and spectrophotometric determination of aluminium(III) in water samples and dialysis concentrates at trace levels with 8-hydroxyquinoline–cobalt(II) coprecipitation system. *J. Hazard. Mater.*, 182, 331-336.